Article

Chinese Science Bulletin

Electronics

June 2012 Vol.57 No.16: 2029–2035
doi: 10.1007/s11434-012-5092-4

Real-time filter based on the quasi-accurate detection of gross errors

LIU Ye[1*], YU AnXi[1], ZHU JuBo[2] & LIANG DianNong[1]

[1] *College of Electronic Science and Engineering, National University of Defense Technology, Changsha 410073, China;*
[2] *Science College, National University of Defense Technology, Changsha 410073, China*

Received December 22, 2011; accepted January 19, 2012

Because of the sensitivity of the Kalman framework to gross errors, proper techniques for detection of gross errors are necessary. By integrating the selection of quasi-accurate observations and the Kalman framework, a new filter called the quasi-accurate filter (QUAF) is developed. The expansibility and implementation scheme of the new algorithm are then discussed in detail, and the reliability matrix for the Kalman filter is proposed to analyze the reliability of the filters with different detection technologies. Finally, the experimental results from a real world case study are used to validate the conclusions. The QUAF carries out the preliminary selection of the quasi-accurate observations (QAOs) using the innovation of the Kalman filter, and use the check QAOs to determine reasonable observations. This causes the QUAF to handle more easily and possess wider expansibility. QUAF can be reformulated to the special cases of several common detection methods, such as the innovation method, robust estimation and quasi-accurate detection (QUAD). Since only reasonable observations are used, the QUAF has better detection accuracy and stronger avoidance of gross errors than the innovation method and robust estimation. Meanwhile, compared with QUAD methods, QUAF introduces the state-predicted model, requiring fewer quasi-accurate observations and making it more suitable for systems with complicated observation structures or sparse observations.

gross error, quasi-accurate detection, Kalman filter, reliability

Citation: Liu Y, Yu A X, Zhu J B, et al. Real-time filter based on the quasi-accurate detection of gross errors. Chin Sci Bull, 2012, 57: 2029–2035, doi: 10.1007/s11434-012-5092-4

There are many definitions for gross error in the literature. A universal viewpoint is that gross errors mean those elements that comprise a small portion of the whole data set and are separated from most of the other elements [1,2]. In surveying, gross errors are often called outliers. At present, most real-time filter systems are based on the Kalman framework [3], such as the extended Kalman filter (EKF), the unscented filter (UKF) and so on [4–6]. Therefore, observations containing gross errors may severely distort the filtered result, or even induce a divergence. That is to say, the mechanism for detecting gross errors must be involved in the actual real-time filter [7].

In most research, the detection of gross errors is often formulated as a hypothesis testing problem based on a detection statistic constructed from the residual errors or the innovations of the filter. The committed steps are the selections of detection criteria and the detection thresholds. Meanwhile, an evaluation of the detection methods should not be ignored.

The detection criteria are obtained by a predictive method. According to the type of information used, the two of methods used here are single channel detection and multi-channel detection. For the single channel detection method, the detection statistic is constructed directly from the predicted observations [2] or from some characteristics of the predicted observations [8,9], which are calculated using temporal correlation of the observations in the same channel. This method requires less calculation and communication, but a drawback is that it does not work when gross errors are present [7]. For the multi-channel detection method, the detection statistic is constructed from the filtered results and is calculated using more than one observed channels [7].

*Corresponding author (email: liuye.cool2007@yahoo.com.cn)

Because more information is used, this method is often superior to the single channel method. If the predicted state is chosen, the detection statistic is constructed only from the filter innovations [10]. Otherwise, if the filter state is chosen, the detection statistic is constructed from the residual errors [11]. Obviously, the current observations are used in the latter method. However, this does not mean more precise detection since the current observations are introduced without considering their quality. Therefore, when the observed geometry is very complex, potential "leverage observations" may induce migration or submergence of gross errors [1].

The detection thresholds are obtained from the confidence interval for the detection statistic. Therefore, it is important to find a detection statistic with good statistical characteristics [12]. This can be achieved by choosing a proper density function to depict the predicted observations, the innovations or the residual errors. To deal with the limitations of the binary editing criteria in the original detection methods, Huber [13] proposed the M-estimator. Many robust filters were also developed, such as the integrated robust filter introduced by Yang et al. [14] for precise orbit determination. Its main drawback is that there is no universal method for constructing the robust function. Ting et al. [15] proposed using the gamma distribution to construct the fusion coefficients and introduced the Expectation-Maximization algorithm to adaptively update the coefficients online. However, the implementation of the algorithm is too complex.

To reduce the effect of "leverage observation", Ou [16] developed a new algorithm called quasi-accurate detection (QUAD). The algorithm considers gross errors to be distinguishable from the estimators of real errors, and resolves the estimators by adding conditions for minimizing the norm of the real errors related to quasi-accurate observations (QAOs). The algorithm is more reliable and prevents migration and submergence of gross errors better than the hypothesis method and some robust schemes, especially in those instances where the observations are severely polluted. [17] Originally, the QUAD method was established as a batch processing scheme and the preliminary selection of QAOs was tightly related to prior observed qualities. Later, ref. [18] extended QUAD to the Kalman framework. This algorithm is restricted to the pre-treatment step and uses the same preliminary selection method as the original QUAD, although there is still a potential migration of gross errors when there is not enough prior information.

Reliability is one of the elemental performance indices of real-time filters. Taking the Kalman filter as an adjustment model, we can introduce reliability theory from the perspective of surveying adjustment, where reliability is defined as the ability of the system to detect errors in the model (gross errors, systematic errors, and so on) and the harmful effect caused by gross errors that have not been detected [1]. Therefore, we can construct a detection criterion for gross errors from the lower bound on model errors that can be detected under a given reliability. The matrix of adjustment factors is used to display the reliability index in traditional adjustment theory [1,19]. Unfortunately, the reliability analysis method cannot be extended to the Kalman filter, where reliability depends on both the observed error and the state predicted error.

This paper focuses on the detection of gross errors in a real-time filter. First, by introducing the predicted state to preliminary selection, the QUAD technique is merged into the Kalman framework. This produces a more reliable filter, which we call the quasi-accurate filter (QUAF). Second, the reliability matrix for the Kalman filter is established referring to reliability theory in the adjustment system. Using the reliability matrix, the filter performance of QUAF is compared with the other three detection algorithms. Finally, two representative examples in trajectory target tracking are given to support our findings.

1 A brief introduction to the quasi-accurate detection method

Consider the following observed system:

$$\boldsymbol{Hx} = \boldsymbol{y} + \boldsymbol{\Delta\sigma}, \tag{1}$$

where $\boldsymbol{x}$ is an m-dimensional state vector, $\boldsymbol{y}$ is the n-dimensional observed vector, $\boldsymbol{H}$ is the observed matrix and $\boldsymbol{\Delta}$ is the real errors related to observations. If we let the coefficient matrix of observations be $\boldsymbol{P}$, then the adjustment factor (reliability matrix) [1] can be calculated as $\boldsymbol{R} = \boldsymbol{I} - \boldsymbol{H}(\boldsymbol{H}^{\mathrm{T}}\boldsymbol{PH})\boldsymbol{H}^{\mathrm{T}}\boldsymbol{P}$. It can be easily obtained that $\boldsymbol{R\Delta} = -\boldsymbol{Ry}$. In QUAD, gross errors are detected according to the estimator of $\boldsymbol{\Delta}$. Suppose that an r-dimensional quasi-accurate observed vector $\boldsymbol{y}_r$ is selected $(r \leqslant n)$. Since $\boldsymbol{R}$ is rank deficient, the rank-deficiency equation for real errors is resolved by adding the condition that the minimum norm of the real errors related to the QAOs is restrained. That is, $\boldsymbol{\Delta}$ is solved by the following equations:

$$\begin{cases} \boldsymbol{R\Delta} = -\boldsymbol{Ry}, \\ \boldsymbol{G}_r\boldsymbol{\Delta}_r = \boldsymbol{0}_{r\times 1}. \end{cases} \tag{2}$$

The gross errors can then be stepwise detected from $\boldsymbol{\Delta}$ according to the "hive-off" phenomenon [16–19].

2 Real-time filter based on quasi-accurate detection

2.1 Algorithm expression

In this section, we merge QUAD into the Kalman framework by carrying out preliminary selection according to the state prediction ability of the filter. This proves to be very effective at improving the reliability of the filter. At time step $k+1$, consider the discrete time system of the form:

$$\begin{cases} \boldsymbol{x}_{k+1} = \boldsymbol{A}_k \boldsymbol{x}_k + \boldsymbol{w}_k, \\ \boldsymbol{y}_{k+1} = \boldsymbol{H}_{k+1}\boldsymbol{x}_{k+1} + \boldsymbol{n}_{k+1}, \end{cases} \tag{3}$$

where the noise vectors $\boldsymbol{w}_k$ and $\boldsymbol{n}_{k+1}$ have a mean of zero, and satisfy $E(\boldsymbol{w}_k\boldsymbol{w}_{kk}^{\mathrm{T}})=\boldsymbol{P}_{\boldsymbol{w},k}$, $E(\boldsymbol{n}_k\boldsymbol{n}_k^{\mathrm{T}})=\boldsymbol{P}_{\boldsymbol{n},k}$ and $E(\boldsymbol{w}_k\boldsymbol{n}_k^{\mathrm{T}})=\boldsymbol{0}$. Taking eq. (3) as an adjustment system, we have $\boldsymbol{\Delta}_{k+1} = -\boldsymbol{n}_{k+1}$ as the real errors. Let $\hat{\boldsymbol{x}}_k$ denote the estimated state with covariance $\boldsymbol{P}_{\boldsymbol{x},k}$ that is obtained at time step k. The Kalman filter uses a forecast-calibration mechanism to obtain a state estimation recursively. This is equivalent to solving the following optimization problem [14,20]:

$$\hat{\boldsymbol{x}}_{k+1} = \min_{\boldsymbol{x}_{k+1}}\{\tilde{\boldsymbol{x}}_{k+1|k}^{\mathrm{T}}\bar{\boldsymbol{P}}_{\boldsymbol{x},k+1}\tilde{\boldsymbol{x}}_{k+1|k} + \tilde{\boldsymbol{y}}_{k+1|k}^{\mathrm{T}}\boldsymbol{P}_{\boldsymbol{n},k}\tilde{\boldsymbol{y}}_{k+1|k}\}, \tag{4}$$

where $\tilde{\boldsymbol{x}}_{k+1|k} = \bar{\boldsymbol{x}}_{k+1|k} - \boldsymbol{x}_{k+1} = \boldsymbol{A}_k\hat{\boldsymbol{x}}_k - \boldsymbol{x}_{k+1}$ is the predicted state error and $\tilde{\boldsymbol{y}}_{k+1|k} = \hat{\boldsymbol{y}}_{k+1} - \boldsymbol{y}_{k+1} = \boldsymbol{H}_{k+1}\hat{\boldsymbol{x}}_{k+1} - \boldsymbol{y}_{k+1}$ is the residual error respectively, and $\bar{\boldsymbol{P}}_{\boldsymbol{x},k+1}$ is the estimated variances of $\tilde{\boldsymbol{x}}_{k+1|k}$.

We calculate the innovation $\boldsymbol{v}_{k+1} = \boldsymbol{y}_{k+1} - \boldsymbol{H}_{k+1}\bar{\boldsymbol{x}}_{k+1|k}$ and select $\boldsymbol{y}_{r,k+1}$ as the preliminary QAOs. Without loss generality, suppose that $\boldsymbol{P}_{\boldsymbol{n},k+1} = [\boldsymbol{P}_{s,k+1}, \boldsymbol{P}_{sr,k+1}; \boldsymbol{P}_{rs,k+1}, \boldsymbol{P}_{r,k+1}]$, $\boldsymbol{y}_{k+1} = [\boldsymbol{y}_{s,k+1}; \boldsymbol{y}_{r,k+1}]$, $\boldsymbol{H}_{k+1} = [\boldsymbol{H}_{s,k+1}; \boldsymbol{H}_{r,k+1}]$, and by reshaping the other component of $\boldsymbol{y}$ to $\boldsymbol{y}_{s,k+1}$. Furthermore, let $\boldsymbol{G}_{r,k+1}$ be the coefficient matrix of $\boldsymbol{y}_{r,k+1}$, and $\boldsymbol{G}_{k+1} = [\boldsymbol{0}_{m\times s}, \boldsymbol{G}_{r,k+1}]$. Then the filter is equivalent to solving the following equations:

$$\begin{cases} \bar{\boldsymbol{P}}_{\boldsymbol{x},k+1}^{-1/2}\boldsymbol{x}_{k+1} = \boldsymbol{P}_{\boldsymbol{x},k+1}^{-1/2}\bar{\boldsymbol{x}}_{k+1|k}, \\ \boldsymbol{P}_{\boldsymbol{n},k+1}^{-1/2}(\boldsymbol{H}\boldsymbol{x}_{k+1} - \boldsymbol{\Delta}_{k+1}) = \boldsymbol{P}_{\boldsymbol{n},k+1}^{-1/2}\boldsymbol{y}_{k+1}, \\ \boldsymbol{G}_{k+1}\boldsymbol{\Delta}_{k+1} = \boldsymbol{0}_{n\times 1}. \end{cases} \tag{5}$$

Let $\boldsymbol{X}_{k+1}=[\boldsymbol{x}_{k+1}^{\mathrm{T}}, \boldsymbol{\Delta}_{k+1}^{\mathrm{T}}]^{\mathrm{T}}$, $\boldsymbol{P}_{\boldsymbol{Q},k+1} = (\boldsymbol{G}_{r,k+1}^{\mathrm{T}}\boldsymbol{G}_{r,k+1})^{-1}$, $\tilde{\boldsymbol{H}}_{k+1} = [-\boldsymbol{H}_{k+1}, \boldsymbol{I}_n]$, $\boldsymbol{B}_{k+1}=[\bar{\boldsymbol{P}}_{\boldsymbol{x},k+1}^{-1/2}, \boldsymbol{0}; \boldsymbol{P}_{\boldsymbol{n},k+1}^{-1/2}\boldsymbol{H}, -\boldsymbol{P}_{\boldsymbol{n},k+1}^{-1/2}; \boldsymbol{0}, \boldsymbol{G}_{k+1}]$, $\boldsymbol{C}_{k+1} = [\bar{\boldsymbol{P}}_{\boldsymbol{x},k}^{-1/2}\bar{\boldsymbol{x}}_{k+1|k}; \boldsymbol{P}_{\boldsymbol{n},k}^{-1/2}\boldsymbol{y}_{k+1}; \boldsymbol{0}_{n\times 1}]$, and $\boldsymbol{I}_n$ be the n-dimensional identity matrix. Then, according to adjustment theory [1], the state can be calculated as

$$\begin{aligned} \hat{\boldsymbol{X}}_{k+1} &= (\boldsymbol{B}_{k+1}^{\mathrm{T}}\boldsymbol{B}_{k+1})^{-1}\boldsymbol{B}_{k+1}^{\mathrm{T}}\boldsymbol{C}_{k+1} \\ &= \left(\begin{bmatrix} \bar{\boldsymbol{P}}_{\boldsymbol{x},k+1}^{-1} & \boldsymbol{0}_{m\times s} & \boldsymbol{0}_{m\times r} \\ \boldsymbol{0}_{s\times m} & \boldsymbol{0}_{s\times s} & \boldsymbol{0}_{s\times r} \\ \boldsymbol{0}_{r\times m} & \boldsymbol{0}_{r\times s} & \boldsymbol{P}_{\boldsymbol{Q},k+1}^{-1} \end{bmatrix} + \tilde{\boldsymbol{H}}_{k+1}^{\mathrm{T}}\boldsymbol{P}_{\boldsymbol{n},k+1}^{-1}\tilde{\boldsymbol{H}}_{k+1}\right)^{-1} \\ &\cdot\begin{bmatrix} \bar{\boldsymbol{P}}_{\boldsymbol{x},k+1}^{-1}\bar{\boldsymbol{x}}_{k+1|k} + \boldsymbol{H}_{k+1}^{\mathrm{T}}\boldsymbol{P}_{\boldsymbol{n},k+1}^{-1}\boldsymbol{y}_{k+1} \\ -\boldsymbol{P}_{\boldsymbol{n},k+1}^{-1}\boldsymbol{y}_{k+1} \end{bmatrix}. \end{aligned} \tag{6}$$

To simplify eq. (6), we refer to the solving technique for compound co-linearity in [21]. Denoting $\delta > 0$ as a small constant and $\boldsymbol{M}_k^{-1} = [\delta\boldsymbol{I}_s, \boldsymbol{0}_{s\times r}; \boldsymbol{0}_{r\times s}, \boldsymbol{P}_{\boldsymbol{Q},k+1}^{-1}]$, we have the following approximate formulas:

$$\begin{aligned} \hat{\boldsymbol{X}}_{k+1} &\approx \left(\begin{bmatrix} \bar{\boldsymbol{P}}_{\boldsymbol{x},k+1}^{-1} & \boldsymbol{0}_{m\times n} \\ \boldsymbol{0}_{n\times m} & \boldsymbol{M}_k^{-1} \end{bmatrix} + \tilde{\boldsymbol{H}}_{k+1}^{\mathrm{T}}\boldsymbol{P}_{\boldsymbol{n},k+1}^{-1}\tilde{\boldsymbol{H}}_{k+1}\right)^{-1} \\ &\cdot\begin{bmatrix} \bar{\boldsymbol{P}}_{\boldsymbol{x},k+1}^{-1}\bar{\boldsymbol{x}}_{k+1|k} + \boldsymbol{H}_{k+1}^{\mathrm{T}}\boldsymbol{P}_{\boldsymbol{n},k+1}^{-1}\boldsymbol{y}_{k+1} \\ -\boldsymbol{P}_{\boldsymbol{n},k+1}^{-1}\boldsymbol{y}_{k+1} \end{bmatrix}. \end{aligned} \tag{7}$$

Letting $\boldsymbol{L}_{k+1} = \boldsymbol{H}_{k+1}\bar{\boldsymbol{P}}_{\boldsymbol{x},k+1}\boldsymbol{H}_{k+1}^{\mathrm{T}} + \boldsymbol{P}_{\boldsymbol{n},k+1} + \boldsymbol{M}_k$ and applying the theorem of matrix inversion [22], eq. (7) can be rewritten as

$$\begin{aligned} \hat{\boldsymbol{X}}_{k+1} &\approx \begin{bmatrix} \bar{\boldsymbol{x}}_{k+1|k} + \bar{\boldsymbol{P}}_{\boldsymbol{x},k+1}\boldsymbol{H}_{k+1}^{\mathrm{T}}\boldsymbol{P}_{\boldsymbol{n},k+1}^{-1}\boldsymbol{y}_{k+1} \\ -\boldsymbol{M}_k\boldsymbol{P}_{\boldsymbol{n},k+1}^{-1}\boldsymbol{y}_{k+1} \end{bmatrix} - \begin{bmatrix} -\bar{\boldsymbol{P}}_{\boldsymbol{x},k+1}\boldsymbol{H}_{k+1}^{\mathrm{T}} \\ \boldsymbol{M}_k \end{bmatrix}\boldsymbol{L}_{k+1}^{-1} \\ &\cdot\left[-\boldsymbol{H}_{k+1}\bar{\boldsymbol{x}}_{k+1|k} - \boldsymbol{H}_{k+1}\bar{\boldsymbol{P}}_{\boldsymbol{x},k+1}\boldsymbol{H}_{k+1}^{\mathrm{T}}\boldsymbol{P}_{\boldsymbol{n},k+1}^{-1}\boldsymbol{y}_{k+1} - \boldsymbol{M}_k\boldsymbol{P}_{\boldsymbol{n},k+1}^{-1}\boldsymbol{y}_{k+1}\right] \\ &= \begin{bmatrix} \bar{\boldsymbol{x}}_{k+1|k} + \bar{\boldsymbol{P}}_{\boldsymbol{x},k+1}\boldsymbol{H}_{k+1}^{\mathrm{T}}\boldsymbol{P}_{\boldsymbol{n},k+1}^{-1}\boldsymbol{y}_{k+1} \\ -\boldsymbol{M}_k\boldsymbol{P}_{\boldsymbol{n},k+1}^{-1}\boldsymbol{y}_{k+1} \end{bmatrix} \\ &- \begin{bmatrix} -\bar{\boldsymbol{P}}_{\boldsymbol{x},k+1}\boldsymbol{H}_{k+1}^{\mathrm{T}} \\ \boldsymbol{M}_k \end{bmatrix}\boldsymbol{L}_{k+1}^{-1}\left[-\boldsymbol{H}_{k+1}\bar{\boldsymbol{x}}_{k+1|k} - \boldsymbol{L}_{k+1}\boldsymbol{P}_{\boldsymbol{n},k+1}^{-1}\boldsymbol{y}_{k+1} + \boldsymbol{y}_{k+1}\right] \\ &= \begin{bmatrix} \bar{\boldsymbol{x}}_{k+1|k} + \bar{\boldsymbol{P}}_{\boldsymbol{x},k+1}\boldsymbol{H}_{k+1}^{\mathrm{T}}\boldsymbol{L}_{k+1}^{-1}\left(\boldsymbol{y}_{k+1} - \boldsymbol{H}_{k+1}\bar{\boldsymbol{x}}_{k+1|k}\right) \\ -\boldsymbol{M}_k\boldsymbol{L}_{k+1}^{-1}\left(\boldsymbol{y}_{k+1} - \boldsymbol{H}_{k+1}\bar{\boldsymbol{x}}_{k+1|k}\right) \end{bmatrix}. \end{aligned} \tag{8}$$

Furthermore, let $\boldsymbol{D}_{k+1} = \boldsymbol{H}_{r,k+1}\bar{\boldsymbol{P}}_{\boldsymbol{x},k+1}\boldsymbol{H}_{r,k+1}^{\mathrm{T}} + \boldsymbol{P}_{r,k+1} + \boldsymbol{P}_{\boldsymbol{Q},k+1}$ and take $\boldsymbol{L}_{k+1}$ as the block form $\boldsymbol{L}_{k+1} = [\boldsymbol{L}_{k+1}^{11}, \boldsymbol{L}_{k+1}^{12}; \boldsymbol{L}_{k+1}^{21}, \boldsymbol{L}_{k+1}^{22}]$, where

$$\begin{cases} \boldsymbol{L}_{k+1}^{11} = \boldsymbol{H}_{s,k+1}\bar{\boldsymbol{P}}_{\boldsymbol{x},k+1}\boldsymbol{H}_{s,k+1}^{\mathrm{T}} + \boldsymbol{P}_{s,k+1} + \delta^{-1}\boldsymbol{I}_s, \\ \boldsymbol{L}_{k+1}^{12} = \boldsymbol{H}_{s,k+1}\bar{\boldsymbol{P}}_{\boldsymbol{x},k+1}\boldsymbol{H}_{r,k+1}^{\mathrm{T}} + \boldsymbol{P}_{sr,k+1}, \\ \boldsymbol{L}_{k+1}^{21} = \boldsymbol{H}_{r,k+1}\bar{\boldsymbol{P}}_{\boldsymbol{x},k+1}\boldsymbol{H}_{s,k+1}^{\mathrm{T}} + \boldsymbol{P}_{rs,k+1}, \\ \boldsymbol{L}_{k+1}^{22} = \boldsymbol{H}_{r,k+1}\bar{\boldsymbol{P}}_{\boldsymbol{x},k+1}\boldsymbol{H}_{r,k+1}^{\mathrm{T}} + \boldsymbol{P}_{r,k+1} + \boldsymbol{P}_{\boldsymbol{Q},k+1}. \end{cases}$$

Then, noting that $\delta^{-1}\boldsymbol{I}_s \approx \boldsymbol{0}_{s\times s}$ and applying the theorem of matrix inversion [22], we have $\boldsymbol{L}_{k+1}^{-1} \approx [\boldsymbol{0}_{s\times n}; \boldsymbol{0}_{r\times s}, \boldsymbol{D}_{k+1}^{-1}]$ and $\boldsymbol{M}_k\boldsymbol{L}_{k+1}^{-1} \approx [\boldsymbol{I}_s, \boldsymbol{H}_{s,k+1}\bar{\boldsymbol{P}}_{\boldsymbol{x},k+1}\boldsymbol{H}_{r,k+1}^{\mathrm{T}}\boldsymbol{D}_{k+1}^{-1}; \boldsymbol{0}_{r\times s}, \boldsymbol{P}_{\boldsymbol{Q},k+1}\boldsymbol{D}_{k+1}^{-1}]$. Therefore, the filter state and real errors can be calculated as follows:

$$\begin{cases} \hat{\boldsymbol{x}}_{k+1} \approx \bar{\boldsymbol{x}}_{k+1|k} + \bar{\boldsymbol{P}}_{\boldsymbol{x},k+1}\boldsymbol{H}_{r,k+1}^{\mathrm{T}}\boldsymbol{D}_{k+1}^{-1}(\boldsymbol{y}_{r,k+1} - \boldsymbol{H}_{r,k+1}\bar{\boldsymbol{x}}_{k+1|k}), \\ \hat{\boldsymbol{\Delta}}_{s,k+1} \approx \boldsymbol{y}_{s,k+1} - \boldsymbol{H}_{s,k+1}\bar{\boldsymbol{x}}_{k+1|k} \\ \qquad - \boldsymbol{H}_{s,k+1}\bar{\boldsymbol{P}}_{\boldsymbol{x},k+1}\boldsymbol{H}_{r,k+1}^{\mathrm{T}}\boldsymbol{D}_{k+1}^{-1}(\boldsymbol{y}_{r,k+1} - \boldsymbol{H}_{r,k+1}\bar{\boldsymbol{x}}_{k+1|k}) \\ \qquad = \boldsymbol{y}_{s,k+1} - \boldsymbol{H}_{s,k+1}\hat{\boldsymbol{x}}_{k+1}, \\ \hat{\boldsymbol{\Delta}}_{r,k+1} \approx \boldsymbol{P}_{\boldsymbol{Q},k+1}\boldsymbol{D}_{k+1}^{-1}(\boldsymbol{y}_{r,k+1} - \boldsymbol{H}_{r,k+1}\bar{\boldsymbol{x}}_{k+1|k}) \\ \qquad = \boldsymbol{P}_{\boldsymbol{Q},k+1}(\boldsymbol{P}_{\boldsymbol{Q},k+1} + \boldsymbol{P}_{r,k+1})^{-1}(\boldsymbol{y}_{r,k+1} - \boldsymbol{H}_{r,k+1}\hat{\boldsymbol{x}}_{k+1}). \end{cases} \tag{9}$$

If the appropriate preliminary selection is done, then the real error will exhibit a "hive off" phenomenon. That is, the real errors related to the observations that are polluted by gross errors will be distinctly larger than the others, allowing us to obtain the check QAOs. After this, the state vector can be calculated by the standard Kalman framework. Finally, we finish the calculations for time step $k+1$ by repeating the QAOs selection and filter step alternately until the convergence condition is satisfied. For the sake of brevity, we call this algorithm the quasi-accurate filter (QUAF) in this paper. The implementation of the QUAF will be given in detail in Section 2.3.

2.2 Several instructions

(1) Accuracy of the filter. In the derivation above, eqs. (7) and (9) both use the approximation $\delta^{-1}\boldsymbol{I}_s \approx \boldsymbol{0}_{s\times s}$ and are contravariant processes. Therefore, the estimated error caused by the approximation is compensated to some extent. The accuracy of the algorithm relies on the accuracy of the state model. An accurate predicted state not only improves the rationality of the preliminary selection and the estimation accuracy of the real error, but also improves the observability of the filter, which usually has a high breakdown point. Otherwise, more preliminary QAOs are needed to reduce the number of false-alarms by the detection.

(2) Extension to nonlinear systems. The problem with applying the Kalman filter to a nonlinear system is the ability to predict the mean and covariance of the quantities to be estimated. Therefore, letting $\boldsymbol{D}_{k+1} = \bar{\boldsymbol{P}}_{y_r,k+1} + \boldsymbol{P}_{Q,k+1}$ and referring to the equations for estimating the covariance and gain matrix in the filter, eq. (9) can be rewritten as:

$$\begin{cases} \hat{\boldsymbol{x}}_{k+1} = \bar{\boldsymbol{x}}_{k+1|k} + \bar{\boldsymbol{P}}_{xy_r,k+1}\boldsymbol{D}_{k+1}^{-1}(\boldsymbol{y}_{r,k+1} - \bar{\boldsymbol{y}}_{r,k+1}), \\ \hat{\boldsymbol{\varDelta}}_{s,k+1} = \boldsymbol{y}_{s,k+1} - \hat{\boldsymbol{y}}_{s,k+1}, \\ \hat{\boldsymbol{\varDelta}}_{r,k+1} \approx \boldsymbol{P}_{Q,k+1}(\boldsymbol{P}_{Q,k+1} + \boldsymbol{P}_{r,k+1})^{-1}(\boldsymbol{y}_{r,k+1} - \hat{\boldsymbol{y}}_{r,k+1}). \end{cases} \quad (10)$$

where $\hat{\boldsymbol{y}}_{k+1} = [\hat{\boldsymbol{y}}_{s,k+1}; \hat{\boldsymbol{y}}_{r,k+1}]$ is calculated from $\hat{\boldsymbol{x}}_{k+1}$, and $\bar{\boldsymbol{P}}_{y,k+1} = [\bar{\boldsymbol{P}}_{y_s,k+1}, \bar{\boldsymbol{P}}_{y_s y_r,k+1}; \bar{\boldsymbol{P}}_{y_r y_s,k+1}, \bar{\boldsymbol{P}}_{y_r,k+1}]$, $\bar{\boldsymbol{P}}_{xy,k+1} = [\bar{\boldsymbol{P}}_{xy_s,k+1}, \bar{\boldsymbol{P}}_{xy_r,k+1}]$ are the corresponding predicted covariance. The advantage of eq. (10) is that most nonlinear filter algorithms can be easily applied to it.

(3) Differences between the algorithm and the standard Kalman filter. On the one hand, the filter gain in eqs. (9) and (10) ($\boldsymbol{K}_{k+1} = \bar{\boldsymbol{P}}_{xy_r,k+1}\boldsymbol{D}_{k+1}^{-1}$) are smaller than that in the standard Kalman filter ($\boldsymbol{K}_{k+1} = \bar{\boldsymbol{P}}_{xy_r,k+1}\bar{\boldsymbol{P}}_{y_r,k+1}^{-1}$). On the other hand, $\hat{\boldsymbol{\varDelta}}_{s,k+1}$ is bigger than the residual calculated from $\hat{\boldsymbol{x}}_{k+1}$, while $\hat{\boldsymbol{\varDelta}}_{r,k+1}$ is smaller than the corresponding residual $\boldsymbol{y}_{r,k+1} - \hat{\boldsymbol{y}}_{r,k+1}$.

(4) Reliability of the algorithm. There are two potential reasons that the QUAF improves the filter reliability. The first is that the QUAF uses some of the observations ($\boldsymbol{y}_{r,k+1}$) to estimate the state $\boldsymbol{x}$, and the observations $\boldsymbol{y}_{s,k+1}$ only affect some of the real errors ($\boldsymbol{\varDelta}_{s,k+1}$) here. Therefore, the QUAF can reduce the effect of "leverage observations" and can detect more than one gross error simultaneously. The other reason is that the introduction of the dynamic model can improve the detection ability of the QUAF. Less than m (the state dimension) observations are needed to solve for the real error here. Therefore, the QUAF has a high breakdown point.

(5) Adaptability of the algorithms. Several commonly used detection algorithms can be considered to be special cases of the QUAF. If no iteration steps are involved, then the QUAF is equivalent to the innovation algorithm. If all the observations are taken as QAOs and an appropriate robust coefficient function is used to select the check QAOs, then the QUAF becomes the robust estimation algorithm. If a state model is not used, i.e. the first equation of X(5)X is not introduced into the detection step, then the QUAF is similar to the original QUAD algorithm.

2.3 Implementation scheme

The key in the QUAF is the selection of the QAOs, which includes the preliminary selection and the check selection. This can be done according to the innovation, the residual and the real error. In the QUAF, the minimum number of QAOs r_0 is determined according to the observability at the current sample step. Then, the QUAF is implemented as follows.

Step 1: Carry out the preliminary selection according to the innovation. Let v_{k+1}^i be the *i*-th element of the innovation, and d^i be the square root of the element in the *i*-th row and *i*-th column of the predicted covariance $\bar{\boldsymbol{P}}_{y_r,k+1}$. Calculate and rank the normalized innovations $\bar{v}_{k+1}^i = |v_{k+1}^i|/d^i$ in numerical order. Then, the smallest r elements are chosen as the preliminary selections.

Step 2: Carry out the check selection according to a "hive off" of the real error. Let l^i be the square root of the element in the *i*-th row and *i*-th column of the observed covariance $\boldsymbol{P}_{y_r,k+1}$. Taking $C = 1.483 med\{|\hat{\varDelta}^1|, \cdots, |\hat{\varDelta}^n|\}$, calculate and rank the detected index $W_i = \hat{\varDelta}^i/[Cl^i]$ in numerical order. Denote the ranked serials as $\bar{W}_j$, where $j = 1, \cdots, n$. Let $\mathrm{d}\bar{W}_j = \bar{W}_{j+1} - \bar{W}_j$, and select the "hive off" point j_0. The selection strategy ensures that there is a large difference in $\mathrm{d}\bar{W}_j$ both above and below the "hive off" point. Then, take the elements below the "hive off" point ($\{\bar{W}_j, j = 1, \cdots, j_0\}$) as the check QAOs.

Step 3: Repeat the filter. Recalculate the state and the real error of the filter using the check QAOs. If there is an obvious change in the "hive off" (the position of j_0 or the elements in the check QAOs $\{\bar{W}_j, j = 1, \cdots, j_0\}$), return to Step 2 and do the check selection again. Otherwise, continue to Step 4.

Step 4: Calculate the estimated state. First, referring to the robust filter [14], construct the equivalent coefficient function. Then calculate the estimated state by carrying out the filter using the check QAOs. Finally, if the state covariance has no obvious change or the maximum number of iterations is reached, the calculation at the current time step is finished. Otherwise, increase the iteration number by 1 and set $r = r - 1$.

Step 5: If $r < r_0$, finish the calculation at the current step time. Otherwise, return to Step 1.

The main differences between the QUAF and the original QUAD are as follows. (1) The innovation is used for the preliminary selection in the QUAF. This can be viewed as prior information about the state model and obviously simplifies the preliminary selection. Meanwhile, the dependence on the prior quality of the instrument or the least square residual is overcome by QUAD. (2) The check selection process is simplified without obvious effect on the filter result, which is verified by examination. (3) The robust filter technique is used to avoid the limitations of the binary editing criteria in the original methods.

One point that should be noted is the filter divergence problem. If the condition $r < r_0$ is satisfied for a long time, the filter performance will depend greatly on the predictive ability of the state model. This may incur the potential risk of filter divergence. Therefore, the technique for judging and treating divergence should also be considered. For the sake of brevity, we will discuss this problem in a separate paper.

3 Reliability analysis

In this section, the reliability analysis method from adjustment theory is extended to the Kalman filter. We use this to compare several commonly used algorithms for the detection of gross errors.

In system(3), the residual after filter implementation is

$$\begin{aligned} \boldsymbol{V}_{k+1} &= -\boldsymbol{R}_{k+1}\boldsymbol{H}_{k+1}\tilde{\boldsymbol{x}}_{k+1|k} - \boldsymbol{R}_{k+1}\boldsymbol{\Delta}_{k+1} \\ &= -\boldsymbol{R}_{k+1}\boldsymbol{H}_{k+1}\tilde{\boldsymbol{x}}_{k+1|k} \\ &\quad -[\boldsymbol{\Delta}_{s,k+1} - \bar{\boldsymbol{P}}_{\boldsymbol{y}_r\boldsymbol{y}_s,k+1}\bar{\boldsymbol{P}}^{-1}_{\boldsymbol{y}_r,k+1}\boldsymbol{\Delta}_{r,k+1}; \boldsymbol{P}_{r,k+1}\bar{\boldsymbol{P}}^{-1}_{\boldsymbol{y}_r,k+1}\boldsymbol{\Delta}_{r,k+1}], \end{aligned} \tag{11}$$

In eq.(11), the first term is determined by the state predicted error and the second term depends on the real error. Since these two terms have the same coefficient matrix, we define $\boldsymbol{R}_{k+1} = \boldsymbol{I}_{n\times n} - \boldsymbol{H}_{k+1}\boldsymbol{K}_{r,k+1}$ to be the reliability matrix of the Kalman filter. The matrix can be rewritten as

$$\boldsymbol{R}_{k+1} = \begin{bmatrix} \boldsymbol{I}_s & -\bar{\boldsymbol{P}}_{\boldsymbol{y}_r\boldsymbol{y}_s,k+1}\bar{\boldsymbol{P}}^{-1}_{\boldsymbol{y}_r,k+1} \\ \boldsymbol{0}_{r\times s} & \boldsymbol{P}_{r,k+1}\bar{\boldsymbol{P}}^{-1}_{\boldsymbol{y}_r,k+1} \end{bmatrix}. \tag{12}$$

We refer to this reliability matrix while discussing the reliability of several other detection algorithms.

(1) Innovation algorithm. When using the innovation algorithm to detect gross errors in the filter, we have $r = 0$, $\boldsymbol{R}_{k+1} = \boldsymbol{I}_n$, and

$$\boldsymbol{V}_{k+1} = -\boldsymbol{H}_{k+1}\tilde{\boldsymbol{x}}_{k+1|k} - \boldsymbol{\Delta}_{k+1}. \tag{13}$$

As we can see, the residual is related to both the state predicted error and the real error. The state predicted error acts on all the observed channels according to the observed geometry, while the real error only acts on the observed channels where it exists. Therefore, the reliability of the innovation algorithm is determined by the predicted state. That is to say, if the state predicted error (3) is small and has a uniform effect on all the observations, we can obtain high reliability by reducing the effect of "leverage observations" in the innovation algorithm. Otherwise, we may produce incorrect detection results.

(2) Robust filter. In the robust filter, we have $r = n$, $\boldsymbol{R}_{k+1} = \boldsymbol{P}_{n,k+1}\bar{\boldsymbol{P}}^{-1}_{\boldsymbol{y},k+1}$, and

$$\boldsymbol{V}_{k+1} = -\boldsymbol{R}_{k+1}\boldsymbol{H}_{k+1}\tilde{\boldsymbol{x}}_{k+1|k} - \boldsymbol{R}_{k+1}\boldsymbol{\Delta}_{k+1}. \tag{14}$$

Obviously, both the state predicted error and the real error can act on the residuals according to the observed geometry. On the one hand, the introduction of observed information into the detection process can decrease the effect of the state model. On the other hand, polluted observations may go against all residuals and result in the migration or submergence of gross errors when there are "leverage observations", especially in systems with complex observed geometry. Therefore, the reliability of the algorithm depends on the design of the robust coefficient function. Unfortunately, there is no universal robust algorithm for this yet.

(3) QUAD algorithm. In the original QUAD algorithm, the number of QAOs satisfies $r \leqslant n$ and the residual can be calculated by

$$\begin{aligned} \boldsymbol{V}_{k+1} &= -\boldsymbol{R}_{k+1}\boldsymbol{\Delta}_{k+1} \\ &= [\boldsymbol{\Delta}_{s,k+1} - \bar{\boldsymbol{P}}_{\boldsymbol{y}_r\boldsymbol{y}_s,k+1}\bar{\boldsymbol{P}}^{-1}_{\boldsymbol{y}_r,k+1}\boldsymbol{\Delta}_{r,k+1}; \boldsymbol{P}_{r,k+1}\bar{\boldsymbol{P}}^{-1}_{\boldsymbol{y}_r,k+1}\boldsymbol{\Delta}_{r,k+1}]. \end{aligned} \tag{15}$$

That is, the residuals are determined by the real error only. Since the algorithm does not need the state model and performs the preliminary selection according to the prior quality of the instrument or the least square residual [16–19], there may be an incorrect selection when no enough prior information is used in the practical system.

(4) QUAF algorithm. In the QUAF, the number of QAOs satisfies $r \leqslant n$ and the residual can be calculated as

$$\begin{aligned} \boldsymbol{V}_{k+1} &= -\boldsymbol{R}_{k+1}\boldsymbol{H}_{k+1}\tilde{\boldsymbol{x}}_{k+1|k} - \boldsymbol{R}_{k+1}\boldsymbol{\Delta}_{k+1} \\ &= -\boldsymbol{R}_{k+1}\boldsymbol{H}_{k+1}\tilde{\boldsymbol{x}}_{k+1|k} \\ &\quad -[\boldsymbol{\Delta}_{s,k+1} - \bar{\boldsymbol{P}}_{\boldsymbol{y}_r\boldsymbol{y}_s,k+1}\bar{\boldsymbol{P}}^{-1}_{\boldsymbol{y}_r,k+1}\boldsymbol{\Delta}_{r,k+1}; \boldsymbol{P}_{r,k+1}\bar{\boldsymbol{P}}^{-1}_{\boldsymbol{y}_r,k+1}\boldsymbol{\Delta}_{r,k+1}]. \end{aligned} \tag{16}$$

As with the robust filter, both the state predicted error and the real error act on the residual according to the observed geometry. The difference is that a gross error only affects residual in the same observed channel. Besides, by acting on the both the preliminary selection and the calculation of the residual, the improvement in the state prediction accuracy implies a potentially large improvement in the reliability of the QUAF.

Information usages of the different algorithms for the detection of gross errors are shown in Figure 1, which clearly shows that the QUAF and the robust filter require more prior information than the other algorithms. Particularly in the QUAF, the observations are carefully selected before being introduced into the detection process. Therefore, the QUAF may have the highest reliability because of the highest usage of prior information. Besides, both QUAD and QUAF use different techniques to select the QAOs (the former uses the quality of the instrument and the latter uses the state model). Therefore, integrating the two algorithms may be a good approach to improve the reliability of the real-time filter.

4 Example applications

In this section, we consider an example of a multi-velocity-measuring trajectory tracking system to validate the algorithm. The simplified UKF algorithm [4–6] and dynamic model [23] are chosen for the filter. The coefficients of the robust filter and the QUAF are constructed according to Yang et al. [14]. The QUAD implementation is similar to that in Chai and Ou [18]. The differences are that it uses prior quality information for the instrument in preliminary selection and includes the check QAOs selection step described in Section 2.3. We take the trajectory calculated by the post-processing method [2] as the reference trajectory. Then, each time step with a big residual can be viewed as a time when a gross error occurs.

The detection results for two typical observations are shown in Table 1. Because QUAD takes the same preliminary selection as the QUAF, the detection result for QUAD is not given in the table. A summary of the results is as follows: (1) There are no gross errors in observation I. All algorithms obtained the correct results except the robust filter. From the maneuvering character analysis, we discover that the target has a stationary trajectory during the period 700–2000, which means that the predicted state used in the innovation algorithm and the QUAF has a quite high accuracy. Meanwhile, the robust filter used here is done without parameter optimization. Therefore, the robust filter has a higher false alarm probability and is less reliable than the innovation algorithm and the QUAF. (2) There are several places where a gross error occurs in observation II. All algorithms obtained detection results with different false alarm rates. Because the target has a high maneuvering character during the period 2100–2200, the innovation algorithm has the highest rate of false alarms. While benefiting from the adaptive adjustment by the QAOs that restricts the influence of the predicted state, the QUAF effectively reduces the migration of gross errors and yields the lowest false alarm rate.

Second, the number of the filter errors beyond the tolerance error is taken as the criterion for a credible performance evaluation. Let M be the tolerance error and t_0 be the convergence time of the filter. Then the criterion is calculated as $q=\sum_{t_k \geqslant t_0}\varphi[\Delta \boldsymbol{x}(t_k)-M]$, where the function $\varphi(x)$ is defined as $\varphi(x)=(x>0)$. As shown in Table 2, the order in terms of filter reliability is QUAF followed by the robust filter and lastly the innovation algorithm. Because QUAD uses the same preliminary selection as the QUAF, the detection results for QUAD are not given in the table. This is entirely consistent with the reliability analysis in Section 3.

Finally, we reduce the number of instruments artificially and compare the reliability of QUAD and QUAF with the observations, assuming that no prior quality of the instruments is known. Therefore, the residuals of the least

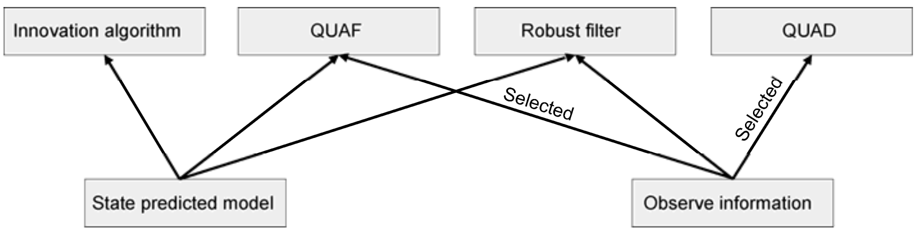

Figure 1 Information usages of different algorithms for the detection of gross errors.

Table 1 Detection results for two typical observations

Position of the gross error	Observation I	Observation II
Innovation algorithm	None	2179, 2180, 2181, 2182, 2183, 2184, 2185, 2186, 2187, 2188, 2189, 2190, 2191, 2192, 2193, 2194, 2195, 2196, 2197, 2198, 2199, 2200, 2201, 2202, 2203, 2204, 2205, 2206, 2207, 2208
Robust filter	793, 884, 1486, 1589	2176, 2177, 2178, 2179, 2180, 2181, 2182, 2183, 2184, 2185, 2186, 2187, 2188, 2189, 2214
QUAF	None	2180, 2181, 2182, 2183, 2184, 2185, 2186, 2188
True position	None	2181, 2182, 2183, 2184, 2185, 2186

Table 2 Number of samples where the filter error is beyond the threshold

	Position (x)	Position (y)	Position (z)	Velocity (x)	Velocity (y)	Velocity (z)
Innovation algorithm	0	0	0	73	155	49
Robust filter	0	0	0	58	144	37
QUAF	0	0	0	60	126	16

square are used for preliminary selection in QUAD. From the calculation results, we conclude that the phenomenon of migration of gross errors occurs in QUAD when the number of instruments is no more than seven. Moreover, QUAD cannot be implemented when fewer than six instruments are used. However, the QUAF can produce nice detection results even if there is no more than six instruments could be used (Referring to the multi-velocity-measuring trajectory tracking example, we need no fewer than six velocity measurements to resolve the trajectory when temporal correlation of the trajectory is not used [24]).

5 Conclusions

The detection of gross errors is an important technique for improving the reliability of real-time filters. By introducing QAOs selection into the Kalman filter process, this paper first develops the QUAF algorithm. Then, the implementation scheme of the new algorithm is established after a discussion of extensions and the adaptability. Finally, the reliability matrix of the Kalman filter is proposed and the performance of the QUAF is compared with three other algorithms. Since it uses the selected observations, the QUAF more successfully prevents the migration or submergence of gross errors. Moreover, the QUAF introduces state predicted information into the preliminary selection process, and is more suitable for complicated systems or poorly validated observations. The QUAF and the reliability analysis method discussed here can be widely used in real-time systems under the Kalman filter framework. However, when the predicted state is unavailable or inaccurate, the QUAF may produce an incorrect detection result. Therefore, introducing other information, such as the prior quality of the instrument, into the QAOs selection may provide useful guidance. This will form part of our ongoing research in this area.

1 Qiu W N, Tao B Z, Yao Y B, et al. The Theory and Method of Surveying Data Processing (in Chinese). Wuhan: Publishing House of Wuhan University, 2008

2 Wang Z M, Yi D Y. Instrumentation Data Modeling and Parameter Estimation (in Chinese). Changsha: Publishing House of the National University of Defense Technology, 1996

3 Lefebrre T, Bruyninckx H, Schutter J D. Kalman filters for nonlinear systems: A comparison of performance. Int J Contr, 2004, 77: 639–654

4 Julier S J, Uhlmann J K. A new extension of the Kalman filter to nonlinear systems. In: The 11th International Symposium on Aerospace/Defense Sensing. Simulation and Controls, Multi Sensor Fusion, Tracking and Resource Management II, FL, US, 1997. 54–65

5 Liu Y, Yu A X, Zhu J B, et al. Unscented Kalman filtering in the additive noise case. Sci China Tech Sci, 2010, 53: 929–941

6 Liu Y, Zhu J B, Hu Z T, et al. Dynamic modeling and simplified UKF for reentry vehicle. In: First Int Congr Image Signal Proc (CISP 2008), Sanya, Hainan, China, 2008. 436–441

7 Yang Y X. Statistics for outlier detection in Kalman filtering (in Chinese). Geo Sci Eng, 2005, 25: 1–4

8 Angiulli F, Basta S, Pizzuti C. Distance-based detection and prediction of outliers. IEEE Trans Knowl Data Eng, 2006, 18: 145–160

9 Xiao Y J, Li J X. Multi-velocity model for outliers restraining and state fusion based on Interacting multi-sensor (in Chinese). Chin J Sci Tech Periodical, 2005, 15: 1106–1112

10 Zhang L, Wang B. Application of H_∞ filtering for outliers restraining in integrated navigation (in Chinese). Trans Beijing Inst Tech, 2009, 29: 600–604

11 Rong S Y, Mu R J, Cui N G. Research on the fault tolerant filter applied on using magnetic magnetometer autonomous navigation (in Chinese). Acta Elec Sin, 2006, 34: 2268–2271

12 Chen K, Gui Q M, Liu L, et al. Robust t-type estimation in Gauss-Markov model (in Chinese). Acta Geo Et Cart Sin, 2008, 37: 281–284, 292

13 Huber P J. Robust Statistics. New York: John Wiley & Sons, 1981

14 Yang Y X, Wen Y L. Integrated robust filter for precise orbit determination. Sci China Earth Sci, 2003, 33: 1112–1119

15 Ting J, Theodorou E, Schaal S. A Kalman filter for robust outlier detection. In: Proc 2007 IEEE/RSJ Int Conf Int Rob Syst, San Diego, CA, USA, 2007. 1514–1519

16 Ou J K. A new method of identifying and locating gross errors—quasi-accurate detection. Chin Sci Bull, 1999, 44: 1777–1781

17 Ou J K. Further on the principle, implementation and application of quasi-accurate detection methods (in Chinese). Eng Survey Map, 2002, 11: 3–6

18 Chai Y J, Ou J K. An improved algorithm for the quality control of Kalman filter (in Chinese). Chin J Sci Tech Periodical, 2004, 14: 904–909

19 Ou J K. On the theory about quality control over surveying data (in Chinese). Eng Survey Map, 2001, 10: 6–10

20 Yang Y, He H, Xu G. Adaptively robust filtering for kinematic geodetic positioning. J Geo, 2001, 75: 109–116

21 Çetin M. Robust model selection criteria for robust Liu estimator. Eur J Oper Res, 2009: 21–24

22 Zhang X D. Matrix Analysis and Application (in Chinese). Beijing: Tsinghua University Press, 2004

23 Li X R, Jilkov V P. A survey of maneuvering target tracking—part II: Ballistic target models. In: Proc 2001 SPIE Conf Signal Data Proc Small Targ, San Diego, CA, USA, 2001. 559–581

24 Liu Y, Zhu J B, Liang D N. Recursive spline filter algorithm for orbit determining utilizing range rate (in Chinese). Signal Proc, 2010, 26: 65–68